CMST 25(1) 31–39 (2019) DOI:10.12921/cmst.2018.0000053

Computation of latent heat in the system of multi-component order parameter: 3D Ashkin-Teller model

D. Jeziorek-Knioła, Z. Wojtkowiak, G. Musiał*

Adam Mickiewicz University
Faculty of Physics
ul. Umultowska 85
61-614 Poznań, Poland
**E-mail: gmusial@amu.edu.pl*

Received: 13 November 2018; revised: 29 March 2019; accepted: 29 March 2019; published online: 31 March 2019

Abstract: The method for computing the latent heat in a system with many independently behaving components of the order parameter proposed previously is presented for a chosen point of the phase diagram of the 3D Ashkin-Teller (AH) model. Binder, Challa, and Lee-Kosterlitz cumulants are exploited and supplemented by the use of the energy distribution histogram. The proposed computer experiments using the Metropolis algorithm calculate the cumulants in question, the internal energy and its partial contributions as well as the energy distribution for the model Hamiltonian and its components. The important part of our paper is an attempt to validate the results obtained by several independent methods.

Key words: the standard 3D Ashkin-Teller model, temperature driven phase transitions, latent heat, high performance computing

I. INTRODUCTION

One of the basic thermodynamic quantities which enables examination of the character of a phase transition is latent heat. In this paper, we propose precise determination of the value of latent heat in the computer experiment based on various cumulants and a histogram of energy distribution. We exploit Binder [1], Challa [2] and Lee-Kosterlitz [3] cumulants as well as the internal energy distribution histogram method [3, 4] which were introduced for systems with one independent order parameter, such as the Ising like models. The non-trivial generalization of the widely exploited Ising model of current interest is the Ashkin-Teller (AT) model [5] which is one of the most important models in statistical physics and every year a dozen works are devoted to it (see e.g. [6–8] and the papers cited therein). Moreover, the AT model shows the complex phase diagram and the Monte Carlo (MC) simulation results published so far suggest the possibility of the occurrence of the non-universal behavior also in the 3D AT model [9–12] which has been observed in the 2D one [13–16].

The AT lattice model has been proposed for four component mixtures [5], but the interest in it significantly increased after Fan's work [17] who expressed it in terms of two Ising models put on the same lattice with spins s_i and σ_i at each lattice site i. As in the original Ising model, we take into account only two-spin interactions of a constant magnitude J_2 between the nearest neighbors. These two independent Ising models are coupled by the four-spin interaction of a constant magnitude J_4, also only between couples of nearest-neighboring spins, leading to the effective Hamiltonian H

$$-\frac{H}{k_B T} = \sum_{[i,j]} \{K_2(s_i s_j + \sigma_i \sigma_j) + K_4 s_i \sigma_i s_j \sigma_j\}. \quad (1)$$

In Eq. (1) $K_n = -J_n/k_B T$, with $n = 2$ or 4, $[i, j]$ denotes summation over nearest-neighboring lattice sites, k_B is the Boltzmann constant, and T is the temperature

of the system. In this paper, we consider the standard 3D AT model put on the cubic lattice. It should be called the standard one as there are many extensions of the AT model.

The cause of the interesting and complex nature of the $K_2(K_4)$ phase diagram of the 3D AT model is the fact that not only two components of the order parameter $\langle s \rangle$ and $\langle \sigma \rangle$ can order independently, but also the product $\langle s\sigma \rangle$ exhibits similar independent behavior, where the symbol $\langle \ldots \rangle$ denotes the thermal average.

The aim of our paper is to provide a method of precise locating the phase transition point and computing the latent heat value in the considered system with multiple components of the order parameter showing an independent order. Our method is based on large-scale computer experiments which exploit the properties of various cumulants. Binder cumulants [1] are based on the order parameter, while the Challa [2] and Lee-Kosterlitz [3] cumulants use the internal energy. Binder cumulants allow for the initial determination of the phase transition region independently for each of the three components of the order parameter. Furthermore, the presence of characteristic minima of the Binder cumulant dependences on the K_2 coupling constant indicates the possibility of occurrence of latent heat for a phase transition [1, 18] at a given coupling constant K_4. Simultaneously, we independently use Challa and Lee-Kosterlitz cumulants, which require adaptation [10, 12] to enable locating the phase transition point for the individual order parameter components and their contribution to the latent heat. Knowing the phase transition point position accurately enough, for strong phase transitions we can determine the latent heat value with a higher precision using the internal energy distribution histogram method [3] adapted to the considered system [4]. A detailed description of the method proposed in this paper and how to systematically validate the results obtained are clarified in Section II.

The method for computing the latent heat proposed in this work will be demonstrated on the example of phase transitions of the first order from the Baxter phase with the ferromagnetic order, where all components of the order parameter are different from zero, to the paramagnetic phase, where all these components are equal to zero. The 3D AT model is convenient for testing the proposed method, since for the case $K_4 = 0$ it reduces to the simple Ising model with the zero latent heat, and at $K_4 = K_2 = 0.157154$ to the 4-state Potts model [9, 10] where we observe the maximum latent heat. To demonstrate the proposed method, we have chosen the point $K_4 = 0.18$, where we observe the intermediate value of the latent heat.

II. OUR COMPUTER EXPERIMENT

We use the MC experiment with importance sampling of states. The finite-size cubic samples of the standard lattice AT model defined in Hamiltonian (1) which are sufficiently large to be able to compute the thermodynamic limit of our results are considered. When performing our MC computer experiments, we compute not only the thermodynamic quantities but also determine their error bars.

In this way, we perform our computer experiments to predict the equilibrium behavior of the 3D standard AT model according to the statistical mechanics methodology [10, 11, 18, 19]. The behavior of our system is fully determined by the Hamiltonian (1). We generate equilibrium configurations (also called microstates) of finite-size cubic spin samples $L \times L \times L$ for fixed values of the model parameters described above at Hamiltonian (1) using the Metropolis algorithm.

The convenient periodic boundary conditions are assumed, as our final results are calculated in the thermodynamic limit. As usual, we first apply thermalization of the length of order of 10^6 Monte Carlo steps (MCS) to bring the system to the thermodynamic equilibrium. At the same time, one MCS in our computer experiment is completed when each of the lattice sites has been visited once. In the case that it is energetically beneficial, the spin is flipped automatically. Otherwise, the probability of the spin-flip is $e^{-2(K_2+K_4)}$.

We split each MC run into k ($6 \leq k \leq 20$) segments called partial averages to determine uncertainties of the computed quantities. One partial average consists from 0.4×10^6 MCS for smallest system sizes up to 3.6×10^6 MCS for the largest L's. However, only every i-th MCS contributes (with $8 \leq i \leq 12$) in the computation of partial averages to avoid correlations between sampled microstates of spins and to sample microstates with the Gibbs probability distribution. Thus, we ensure that our program spends most of time working with states giving the largest contribution to the computed quantities.

It is worth noting that our MC computer experiments take from 20 hours for smallest L's up to a couple of weeks for the largest L values considered when applying sequential processing. Hundreds of such runs have been executed to complete the results of this paper.

We fix the particular value of K_4 coupling and analyze the Binder cumulant $Q_{\alpha,L}(K_2)$ dependences (see e.g. [1, 20, 21])

$$Q_{\alpha,L} = \frac{\langle M_\alpha^2 \rangle_L^2}{\langle M_\alpha^4 \rangle_L}, \tag{2}$$

to pre-locate a temperature-driven phase transition point. Here $\langle M_\alpha^n \rangle_L$ denotes the n-th power of the order parameter of α degrees of freedom, with $\alpha = s$, σ or their product $s\sigma$, which are averaged over an ensemble of independent samples of the size $L \times L \times L$ in agreement with the statistical physics methodology mentioned above. These $Q_{\alpha,L}(K_2)$ dependences intersect mutually around the critical point $K_{2,c}$ for different L values, because for $L_1 < L_2$ and at $K_2 < K_{2,c}$ one obtains $Q_{\alpha,L_1}(K_2) >$

$Q_{\alpha,L_2}(K_2)$, while at $K_2 > K_{2,c}$ there occurs $Q_{\alpha,L_1}(K_2) < Q_{\alpha,L_2}(K_2)$ [1, 20–22]. This is the method for initial localization of the critical K_2 value which is applicable for both continuous and first order phase transition points.

For more precise estimation of a phase transition point position as well as calculation of the latent heat value, we compute also the Challa [2]

$$V_{\alpha,L} = 1 - \frac{\langle E_\alpha^4 \rangle_L}{3\langle E_\alpha^2 \rangle_L^2} \tag{3}$$

and the Lee-Kosterlitz [3]

$$U_{\alpha,L} = \frac{\langle E_\alpha^2 \rangle_L}{\langle E_\alpha \rangle_L^2} \tag{4}$$

like cumulants. In Eqs (3) and (4) $\langle E_\alpha^n \rangle_L$ is the n-th moment of the interaction energy of α-degrees of freedom ($\alpha = s$, σ or their product $s\sigma$) in Hamiltonian (1) separately, which is averaged over an ensemble of independent samples of the size $L \times L \times L$. The Challa and Lee-Kosterlitz cumulants have been adapted [4, 10] by taking not only the whole Hamiltonian (1) for energy E as originally proposed by Challa et al. [2] and by Lee and Kosterlitz [3], but also the Hamiltonian individual terms to be able to compute the latent heat for each component of the order parameter separately [10, 12, 19]. Of course, we make sure that the latent heat l_H computed on the basis of the whole Hamiltonian (1) is equal to the sum of the latent heats l_α ($\alpha = s$, σ or their product $s\sigma$) coming from α degrees of freedom within their error bars.

A phase transition is qualified as continuous when $V_{\alpha,L} = 2/3$ and $U_{\alpha,L} = 1$ in their thermodynamic limits within the respective error bars [2, 3, 10, 12, 19]. For the error bar values of the extremes of these cumulants, we assume the maximum deviation of the points determined in our MC experiments from the fitted curves [10], as the uncertainties should always be rounded up. So, we conclude that when the thermodynamic limit $V_{\alpha,L}^{\min}$ value with its error bar remains different from 2/3 and $U_{\alpha,L}^{\max}$ value with its error bar remains different from 1, a phase transition is qualified to be of the first order [2, 3, 10, 18, 19]. Also locations of minima $K_{2,\alpha}^{\min}$ and maxima $K_{2,\alpha}^{\max}$ scale linearly versus L^{-3} [2, 3, 10, 23]. So, we extrapolate them to the thermodynamic limit. These limit values are better estimations of the critical K_2 value than the ones obtained from the above-mentioned intersection region of the Binder cumulant $Q_{\alpha,L}(K_2)$ dependences.

The partial latent heat l_α coming from the above-mentioned interaction energy E_α of α-degrees of freedom in the limit $L \to \infty$

$$l_\alpha = E_{\alpha,+} - E_{\alpha,-}, \tag{5}$$

where $E_{\alpha,\pm} = E_\alpha(K_2 \to K_{2,c}|_\pm)$, are determined on the basis of the Lee-Kosterlitz formula [3, 12, 23, 24]

$$V_{\alpha,L}^{\min} = \frac{2}{3} - \frac{1}{12}\left(\frac{E_{\alpha,+}}{E_{\alpha,-}} - \frac{E_{\alpha,-}}{E_{\alpha,+}}\right)^2 + \frac{A_V}{L^3} \tag{6}$$

and using the method proposed in [10]. Derivation of this equation [3] uses general thermodynamic properties and is not limited to a specific form of the expression for energy. Here $K_{2,c}$ is the critical value of K_2 coupling at the fixed value of K_4. The quantity A_V in Eq. (6) stands for L independent complicated expression [3]. Thus, Eq. (6) allows us to determine $V_{\alpha,\infty}^{\min}$ limit value using the linear regression to analyze our $V_{\alpha,\infty}^{\min}(L^{-3})$ computer experiment data. This is a powerful tool and similar analysis has been recently applied respectively to the first order phase transitions with an exponential low temperature phase degeneracy [25].

According to the method proposed in [10], one can compute the value E_- by equating this $V_{\alpha,\infty}^{\min}$ value to the first term on the right hand side of Eq. (6) and using the value E_+ estimated from the $E_{\alpha,L}(K_2)$ energy plot for the finite-size samples. When we calculate the values of E_+ and E_-, then l_α value can be obtained from Eq. (5).

It is worth noting that to calculate the latent heat l_α for weak phase transitions of the first order we could use the approximation of Challa et al. [2, 19], which is an alternative to Eq. (6). The results of our computations indicate that although Eq. (6) has been derived for strong phase transitions, it gives correct results also for the weak ones.

In a similar way, we determine the latent heat l_α using our $U_{\alpha,L}$ cumulant maxima values scaled to the thermodynamic limit for each component of the order parameter independently, as well as for the whole system, using the Lee-Kosterlitz formula [3]

$$U_{\alpha,L}^{\max} = \frac{(E_{\alpha,+} + E_{\alpha,-})^2}{4E_{\alpha,+}E_{\alpha,-}} + \frac{A_U}{L^3}, \tag{7}$$

where A_U stands for L independent complicated expression. Obviously, when the latent heat l_α tends to zero, $V_{\alpha,\infty}^{\min}$ approaches the value $2/3$ and $U_{\alpha,\infty}^{\max}$ approaches the value 1, as described above for continuous phase transitions.

For sufficiently strong first order phase transitions, a characteristic histogram of the internal energy E distribution with two peaks in the close critical region can be observed [3, 4]. For samples of finite-size L, the maxima of these peaks appear at the energy value $E_{-,L}$ for the ordered state and at $E_{+,L}$ for the unordered one and they are separated by the minimum of $E_{m,L}$ value. From the technical point of view, the histogram is computed by dividing the range of all internal energy E values (in units of k_BT) appearing in our computer experiments into small subintervals and our program counts the energy occurrence in the individual subintervals. Thus, dividing the received individual values within these intervals by their sum, we get the probability P of the energy E appearance in the system of the finite size L^d, with dimensionality $d = 3$ here. As in the case

of cumulants, the $P_L(E_\alpha, \beta)$ values are calculated independently for each degree of freedom $\alpha = s$, σ, or their product $s\sigma$, and also for the whole Hamiltonian (1), at a critical value $K_{2,c}$ of the parameter K_2 precisely determined from the above mentioned analyzes using cumulants at a fixed value of K_4. Here $\beta = 1/k_BT$. It is worth noting that for continuous phase transitions only a single peak of the probability $P(E)$ dependence appears.

This is the method for precise determination of the phase transition point and the latent heat. We carefully check whether the results we have received independently on the basis of some cumulants based on the order parameter and on the other ones based on internal energy, as well as using the internal energy distribution histogram, are consistent within error bars. However, it is important to verify the correctness of the assumptions about the relations between the cumulants and the values $E_{\alpha,\pm}$ in the macroscopic limit.

III. THE RESULTS AND CONCLUSIONS

As explained in Sections I. and II., we have pre-located the temperature-driven phase transition point at fixed value of the coupling $K_4 = 0.18$ from the intersection points of the Binder cumulant [1, 22] curves $Q_{\alpha,L}(K_2)$ specified by Eq. (2) [10, 20]. In Fig. 1 there appears the region at $K_{2,c} = 0.1452(2)$ where $Q_{\alpha,L}(K_2)$ curves intersect in such a way that for $L_1 < L_2$ and at $K_2 < K_{2,c}$ one has $Q_{\alpha,L_1}(K_2) > Q_{\alpha,L_2}(K_2)$, while at $K_2 > K_{2,c}$ there is $Q_{\alpha,L_1}(K_2) < Q_{\alpha,L_2}(K_2)$, as explained below Eq. (2). The analyses have been performed independently for $\langle\alpha\rangle$ components of the order parameter with $\alpha = s$, σ and $s\sigma$ (see e.g. [10, 20, 21]) allowing us to estimate at least four decimal digits of the K_2 coupling critical value. The intersection region should be identified with the transition from the paramagnetic to the Baxter phase.

The characteristic minimum in the dependence $Q_{s,L}(K_2)$, for clarity in Fig. 1 demonstrated for $L = 22$ only, should be attributed to the first order phase transition [2]. Obviously, the existence of these minima is an important signal, but *not the proof* of the presence of the latent heat, which was discussed in the paper [18].

The essential element for this paper is to demonstrate the proposed way of computation the latent heat of considered phase transitions in 3D AT model which is the system with three behaved independently components of the order parameter. For this purpose we propose first to exploit the Challa like $V_{\alpha,L}$ cumulants properties explained in Section II.

The example of such analyses is shown in Fig. 2 at the fixed value of the coupling K_4=0.18 where the temperature-driven transition from ferromagnetically ordered phase to the disordered one takes place. For clarity we have plotted our results only for selected values of the system linear size L. Characteristic local minima are observed in Fig. 2. To average the scatter of the results and determine more precisely the ordinates $V_{s,L}^{\min}$ and the abscissas $K_{2,L}^{\min}$ of these minima in Fig. 2, our MC computer experiment data were approximated by a polynomial of fourth degree as explained in the caption. Nevertheless, the uncertainties of the ordinates and of the abscissas in Fig. 2 fully take into account this scatter as the uncertainties should always be rounded up.

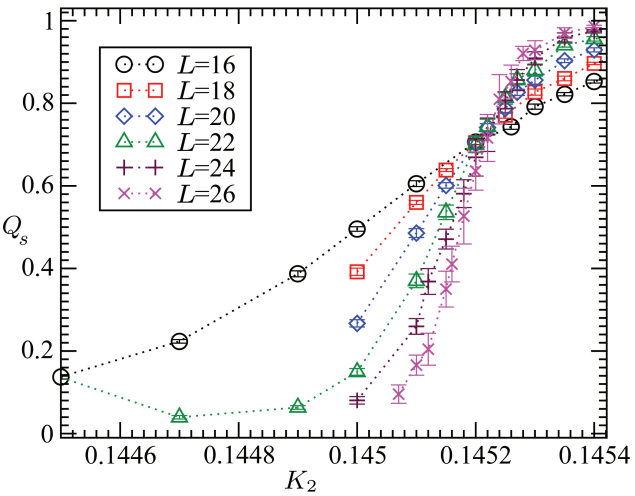

Fig. 1. The Binder cumulants $Q_{\alpha,L}(K_2)$ dependences for $\alpha = s$ and for the system size L values specified in the legend box at the fixed value $K_4 = 0.18$. For clarity of the graph, especially in the intersection region, the minimum for $L = 22$ is only presented. The results of our MC computer experiments are denoted by symbols

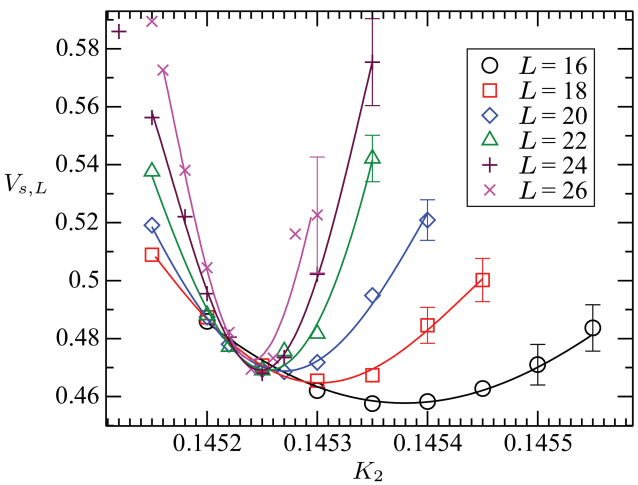

Fig. 2. The dependences $V_{s,L}(K_2)$ with characteristic minima for system sizes L listed in the legend box and at critical coupling $K_4 = 0.18$. The results of our MC computer experiments are denoted by symbols. For the sake of clarity, the error bars of selected points have only been marked. Our MC computer experiment data are approximated by a polynomial of fourth degree (solid curves) to average the scatter of the results

To compute the latent heat, we have to estimate the value of the cumulant $V_{s,L}$ minimum in the thermodynamic limit. For this purpose we have analyzed $V^{\min}_{\alpha,L}(L^{-3})$ dependences using linear regression as explained in Section II. below Eq. (6). The finite-size-scaling analysis of the ordinates $V^{\min}_{s,L}$ is illustrated in Fig. 3 for $\alpha = s$ (the results for $\alpha = \sigma$ are similar because of the symmetry of the Hamiltonian (1)), for $\alpha = s\sigma$, and taking the whole Hamiltonian H for energy E, as explained in the legend box. We see the clear linear character of the MC computer experiment data which are inter- and extrapolated using linear regression. The thermodynamic limit values of the minima of cumulants $V_{\alpha,L}$ are found at the intersection points of these approximating lines with the ordinate axis.

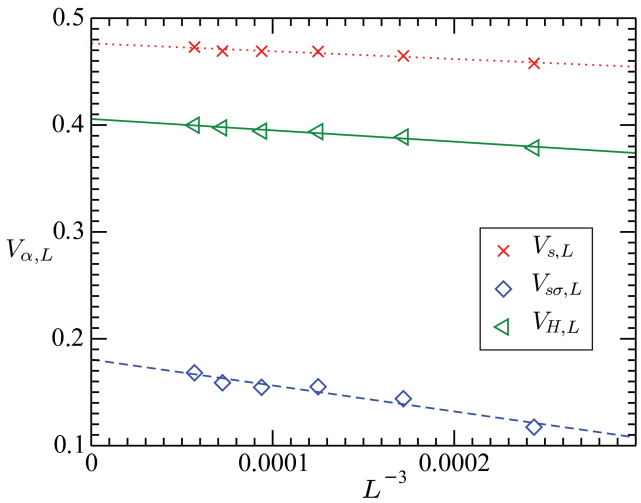

Fig. 3. The values of Challa like cumulants $V^{\min}_{\alpha,L}$ minima extrapolated to the thermodynamic limit for $\alpha = s$ (the dotted line), for $\alpha = s\sigma$ (the dashed line) and taking the whole Hamiltonian H for energy E (the solid line) at the fixed value of the coupling $K_4 = 0.18$ as explained in the legend box. The dependences are fitted by straight lines using the linear regression. The error bars are of order of magnitude of symbols

We have determined the $E_- = 0.093(4)$ value associated with $\langle s \rangle$ component of the order parameter at $K_4 = 0.18$ by comparing the $V^{\min}_{s,\infty} = 0.476(4)$ value to the linear term in Eq. (6) and taking the value $E_+ = 0.187(3)$ estimated from the $E_{s,L}(K_2)$ energy plot for the finite-size samples (see the left-hand graph in Fig. 7 discussed below). It is worth noting that although such an estimation of the step change in the energy value in the thermodynamic limit is very imprecise, it allows the initial calculation of the values E_+ and E_- and a qualitative verification of the location of this energy value jump from E_+ to E_- in the background of the course of the dependence $E_{s,L}(K_2)$. In addition, we find that such a calculated E_- value weakly depends on the precision of estimation of E_+ value varying by a few on the last decimal digit only. Substituting the obtained E_+ and E_- values to Eq. (5) we have obtained $l_s = 0.094(4)$ in k_BT units. Similar analyses have been performed for $\langle s\sigma \rangle$ component of the order parameter and taking the whole Hamiltonian H for energy E, as explained in the legend box in Fig. 3. The results of these analyses are summarized in the second column of Tab. 1.

Tab. 1. The cumulants $V_{\alpha,L}(K_2)$ dependences minima ordinates $V^{\min}_{s,L}$ and abscissas $K_2^{\min}$ as well as the cumulants $U_{\alpha,L}(K_2)$ dependences maxima ordinates $U^{\max}_{s,L}$ and abscissas $K_2^{\max}$ in their thermodynamic limits at $K_4 = 0.18$. α specified in the first column denotes degrees of freedom s (the same value for σ for the Hamiltonian (1) symmetry reasons), or the product $s\sigma$, and H indicates that the whole Hamiltonian H has been taken for the energy E

α	$V^{\min}_{\alpha,\infty}$	$K^{\min}_{2,\infty}$	$U^{\max}_{\alpha,\infty}$	$K^{\max}_{2,\infty}$
s (or σ)	0.476(4)	0.145189(35)	1.128(2)	0.145192(28)
$s\sigma$	0.181(14)	0.145183(38)	1.283(4)	0.145187(25)
H	0.406(5)	0.145195(33)	1.169(4)	0.145187(33)

In order to confirm the correctness of the computation of the latent heat value independently, we have used the properties of the Lee-Kosterlitz like $U_{\alpha,L}$ cumulants as explained in Section II. We did the analyses of $U_{\alpha,L}$ properties in an analogous manner to the above for the cumulants $V_{\alpha,L}$. Fig. 4 illustrates the example of characteristic local $U_{\alpha,L}$ maxima as a function of K_2 coupling at the fixed value of the coupling $K_4 = 0.18$. For clarity, here also we have plotted our results only for selected values of system linear size L. To average the scatter of the results and determine more precisely the ordinates $U^{\max}_{s,L}$ and the abscissas $K^{\max}_{2,L}$ of these maxima in Fig. 4, our MC computer experiment data were also approximated by a polynomial of fourth degree as explained in the caption.

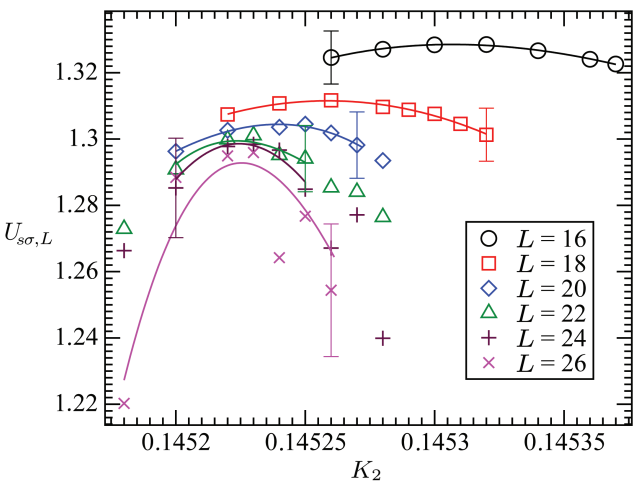

Fig. 4. The dependences $U_{s\sigma,L}(K_2)$ with characteristic maxima for system sizes L listed in the legend box and at critical coupling $K_4 = 0.18$. The results of our MC computer experiments are denoted by symbols. For the sake of clarity, the error bars of selected points have only been marked. Our MC computer experiment data are approximated by a polynomial of fourth degree (solid curves) to average the scatter of the results

Fig. 5 shows the example of computing of the cumulants $U_{\alpha,L}$ maxima values ($\alpha = s$, $s\sigma$ and H denotes taking the whole Hamiltonian H for energy E) in the thermodynamic limit using linear regression as explained in Section II. below Eq. (7). Also here one can see the clear linear character of the MC computer experiment data which are inter- and extrapolated using linear regression.

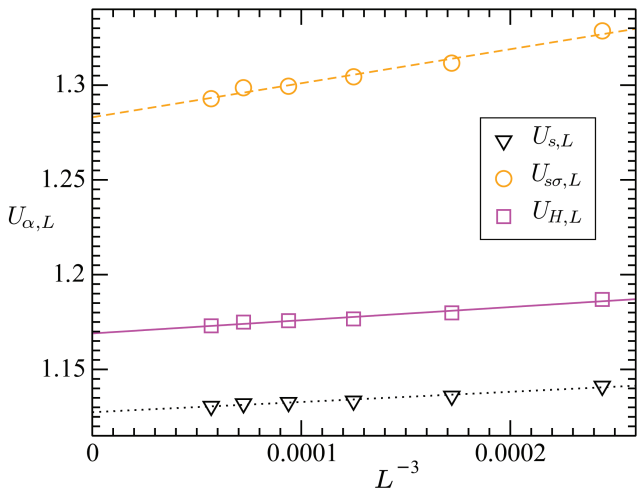

Fig. 5. The values of Lee-Kosterlitz like cumulants $U^{\max}_{\alpha,L}$ maxima extrapolated to the thermodynamic limit for $\alpha = s$ (the dotted line), for $\alpha = s\sigma$ (the dashed line) and taking the whole Hamiltonian H for energy E (the solid line) at the fixed value of the coupling $K_4 = 0.18$ and for degrees of freedom α explained in the legend box. The dependences are fitted by straight lines using the linear regression

The $E_- = 0.073(3)$ value associated with $\langle s\sigma \rangle$ order parameter for $K_4 = 0.18$ has been determined by comparing the $U^{\max}_{s\sigma,\infty} = 1.283(4)$ value to the linear term in Eq. (7) and taking the value $E_+ = 0.202(2)$ estimated from the $E_{s\sigma,L}(K_2)$ energy plot for the finite-size samples. Substituting the obtained E_+ and E_- values to Eq. (5) we have obtained $l_{s\sigma} = 0.129(3)$ in k_BT units. Similar analyses have been performed for $\langle s \rangle$ component of the order parameter and taking the whole Hamiltonian H for energy E, as explained in the legend box in Fig. 5. The results of these analyses are summarized in the fourth column of Tab. 1.

Abscissas $K^{\min}_{2,L}$ of the $V_{\alpha,L}(K_2)$ dependence minima [2] shown in Fig. 2 and abscissas $K^{\max}_{2,L}$ of the $U_{\alpha,L}(K_2)$ dependence maxima [3] illustrated in Fig. 4 for degrees of freedom $\alpha = s$, the product $s\sigma$ and taking the whole Hamiltonian H for energy E, as indicated in the indices of the respective cumulants in the legend box, at the fixed value of the coupling $K_4 = 0.18$, also are linearly correlated versus L^{-3} as shown in Fig. 6. Scaling the positions of these extremes to the thermodynamic limit allowed us to determine more precisely the location of the phase transition, i.e. the critical value of K_2, as explained below Eqs (3) and (4) in Section II. The $K^{\min}_{2,\infty}$ and $K^{\max}_{2,\infty}$ values of these analyses ale collected in the third and fifth columns of Tab. 1, respectively. The critical K_2 value determined on the basis of intersections of the cumulant $Q_{s,L}$ dependencies shown in the right hand graph of Fig. 2 is $K_2 = 0.1452(2)$ as mentioned above. The values obtained by scaling the positions of cumulants $V_{\alpha,L}$ minima and of cumulants $U_{\alpha,L}$ maxima shown in Fig. 6 gave us more accurate average critical value $K_2 = 0.145189(12)$. All obtained K_2 critical values are consistent within the error bars. As we see in Tab. 1, the analyses performed for $U_{\alpha,L}$ cumulants gave us almost the same results as those for $V_{\alpha,L}$ cumulants.

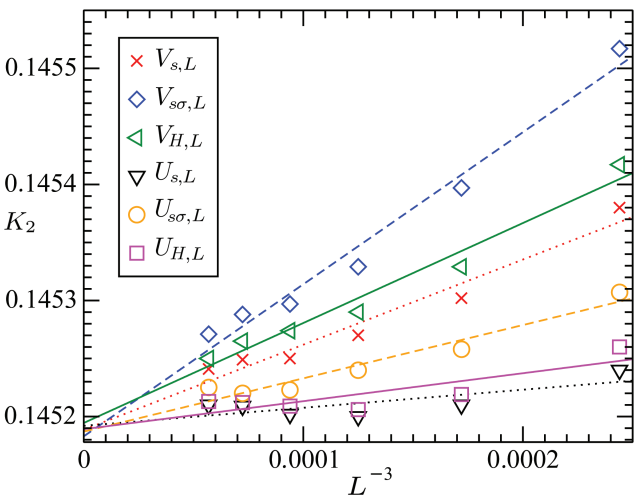

Fig. 6. The values of abscissas $K^{\min}_2$ (diamonds) and $K^{\max}_2$ ($\times$ symbols) of the cumulant $V_{\alpha,L}$ minima and $U_{\alpha,L}$ maxima, respectively, extrapolated to the thermodynamic limit for $\alpha = s$ (the line for $\alpha = \sigma$ falls within the line thickness), $\alpha = s\sigma$, and taking the whole Hamiltonian H for energy E at the fixed value $K_4 = 0.18$, as indicated in the indices of the respective cumulants in the legend box. The dependences are fitted by straight lines using the linear regression

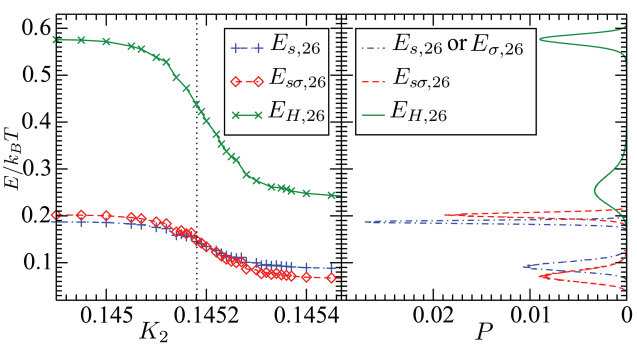

Fig. 7. The the internal energy E (left) and its distribution histogram (right) for $L = 26$ at the phase transition point with $K_4 = 0.18$ and $K_{2,c} = 0.145189$. The right hand graph shows two probability $P_{\alpha,L}$ peaks for degrees of freedom $\alpha = s$ (or $s\sigma$), or the product $s\sigma$, and taking the whole Hamiltonian H for energy E, as indicated in the indices of the respective energies in the legend boxes

We have obtained the completely independent confirmation of correctness and the increased accuracy of our results thanks to the internal energy E_α distribution histogram analyses, whose example is illustrated in Fig. 7 for the system size $L = 26$ at the point $K_4 = 0.18$ and $K_{2,c} = 0.145189(12)$. This is the phase transition point precisely determined as the average value from the third and fifth column of Tab. 1. The degrees of freedom α are given in the legend box. For all degrees of freedom one can see two distinct probability $P_{\alpha,L}$ peaks corresponding to the energies $E_{-,L}$ and $E_{+,L}$, for the ordered and unordered state, respectively, as explained in the last paragraph of Section II.

These two probability $P_{\alpha,L}$ peaks correspond to the minima of the $-\ln P_{\alpha,L}(E_{\alpha,L})$ function [3]. As for the cumulants $V_{\alpha,L}$ minima, we first determine the energy values corresponding to the lower minima $E_{\alpha,-,L}$ for the ordered state and to the upper minima $E_{\alpha,+,L}$ for unordered state for a finite system size L and for degrees of freedom $\alpha = s$ (or σ), the product $s\sigma$, and also taking the whole Hamiltonian H for the energy E.

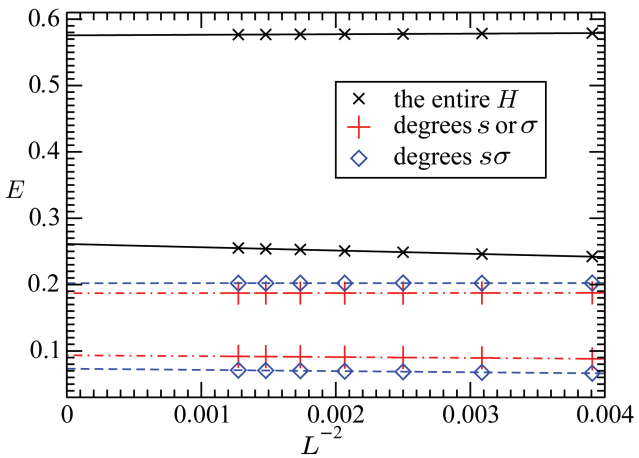

Fig. 8. Values of $E^{\min}_{+,L}$ (upper lines) and $E^{\min}_{-,L}$ (lower lines) of the minima positions of dependencies $-\ln P_L(E_\alpha, \beta)$ received at $K_4 = 0.18$ and $K_{2,c} = 0.145189$ for the system of the finite size L and for degrees of freedom explained in the legend box. The individual lines are extrapolated to their thermodynamic limits E_+ or E_- using linear regression

Fig. 8 shows the results of our analyzes for the energy $E_{\alpha,-,L}$ (lower lines) and $E^{\min}_{\alpha,+,L}$ (upper lines) of the whole Hamiltonian (1), for energy of interaction of degrees of freedom s (the same result is for σ) and the product $s\sigma$ separately, explained in the legend box, for systems with different sizes $16 \le L \le 28$ at the point $K_4 = 0.18$ and $K_{2,c} = 0.145189(12)$. The values $E_{\alpha,-,L}$ and $E_{\alpha,+,L}$ in the L^{-2} function scale linearly to the respective bulk values $E_{\alpha,-}$ and $E_{\alpha,+}$ [3, 4, 12]. Therefore, the individual lines in Fig. 8 were extrapolated to the thermodynamic limit using linear regression. The resulting values $E_{\alpha,-}$ and $E_{\alpha,+}$ after substituting into equation (5) at $K_4 = 0.18$ gave latent heat l_α values collected in the fourth column of Tab. 2 for degrees of freedom α explained in the first column calculated on the basis of cumulants indicated in the second and third columns, as well as using the internal energy distribution histogram shown in the fourth column. The fourth row shows the latent heat summed up over all degrees of freedom, whereas the fifth row presents the latent heat computed for the entire system, i.e. obtained by taking the whole Hamiltonian H for energy E. These results in the fourth and fifth row of the fourth column are consistent within their error bars as we expected.

Tab. 2. The latent heat l_α values for degrees of freedom α explained in the first column calculated on the basis of cumulants indicated in the second and third columns, as well as using the internal energy distribution histogram shown in the fourth column for the coupling $K_4 = 0.18$. The fourth row shows the latent heat summed up over all degrees of freedom, whereas the fifth row presents the latent heat computed for the entire system, i.e. obtained by taking the whole Hamiltonian H for energy E

	U_α	V_α	$-\ln P_\alpha$
l_s (or l_σ)	0.0941(5)	0.0940(6)	0.0935(8)
$l_{s\sigma}$	0.1292(7)	0.1293(8)	0.1289(10)
$l_s + l_\sigma + l_{s\sigma}$	0.3174(17)	0.3173(20)	0.3159(26)
l_H	0.3172(26)	0.3163(19)	0.3145(13)

Using the values $E_{\alpha,+}$ determined on the basis of the internal energy distribution histogram, the cumulant $U_{\alpha,L}$ and $V_{\alpha,L}$ values scaled to their thermodynamic limits on the basis of Eqs (6) and (7), respectively, we have performed calculations of $E_{\alpha,-}$ and of the latent heat l_α. The results obtained using this method are more accurate than those discussed above, for which we have used the value $E_{\alpha,+}$ estimated from the energy plot for a finite-size samples, and are summarized in the second and third column of Tab. 2. These results are consistent with those obtained using the energy distribution histogram (fourth column of Tab. 2) within the error bars. Particularly noteworthy is the very good consistency of the latent heat summed up after individual degrees of freedom (the fourth row) with that obtained for the whole Hamiltonian (1) (the fifth row).

Thus, the method for computation of latent heat, which based on Binder, Challa, and Lee-Kosterlitz like cumulants as well as the energy distribution histogram, has been carefully checked and can successfully be used in systems with many components of an order parameter showing individual ordering.

At the end it is worth noting that Eq. (6) has been derived for strong phase transitions [3]. Thus, to calculate the latent heat l_α for weak phase transitions of the first order, one should use the approximation of Challa et al. [2], which is an alternative to Eq. (6). However, we have checked that although Eq. (6) has been derived for strong phase transitions, our analyzes show that it gives correct results for both

the strong and the weak ones. The latter show a good agreement with the results obtained by us using the Challa approximation.

Acknowledgment

Numerical calculations were carried out on computing platforms of Poznań Supercomputing and Networking Center as well as of Faculty of Physics at Adam Mickiewicz University in Poznań. The authors wish to thank Professors H.T. Diep and J. Rogiers for valuable discussions.

References

[1] K. Binder, D.P. Landau, *Finite-size scaling at first-order phase transitions*, Phys. Rev. B **30**, 1477 (1984).

[2] M.S.S. Challa, D.P. Landau, K. Binder, *Finite-size effects at temperature-driven first-order transitions*, Phys. Rev. B **34**, 1841 (1986).

[3] J. Lee, J.M. Kosterlitz, *Finite-size scaling and Monte Carlo simulations of first-order phase transitions*, Phys. Rev. B **43**, 3265 (1991).

[4] D. Jeziorek-Knioła, Z. Wojtkowiak, G. Musiał, *Computation of Latent Heat based on the Energy Distribution Histogram in the 3D Ashkin-Teller Model*, Acta Phys. Polon. A **133**, 435 (2018).

[5] J. Ashkin, E. Teller, *Statistics of two-dimensional lattices with four components*, Phys. Rev. **64**, 178 (1943).

[6] J.P. Santos, F.C.S. Barreto, *Upper Bounds on the Critical Temperature of the Ashkin-Teller Model*, Braz. J. Phys. **46**, 70 (2016).

[7] Ü. Akıncı, *Nonequilibrium phase transitions in isotropic Ashkin-Teller model*, Physica A **469**, 740 (2017).

[8] J.P. Santos, D.S. Rosa, F.C.S. Barreto, *New Baxter phase in the Ashkin-Teller model on a cubic lattice*, Phys. Lett. A **382**, 272 (2018).

[9] R.V. Ditzian, J.R. Banavar, G.S. Grest, L.P. Kadanoff, *Phase diagram for the Ashkin-Teller model in three dimensions*, Phys. Rev. B **22**, 2542 (1980).

[10] G. Musiał, *Monte Carlo analysis of the tricritical behavior in a three-dimensional system with a multicomponent order parameter: The Ashkin-Teller model*, Phys. Rev. B **69**, 024407 (2004).

[11] G. Musiał, J. Rogiers, *On the possibility of nonuniversal behavior in the 3D Ashkin-Teller model*, Phys. Status Solidi B **243**, 335 (2006).

[12] Z. Wojtkowiak, G. Musiał, *Wide crossover in the 3D Ashkin-Teller model*, Physica A **513**, 104 (2019).

[13] R.J. Baxter, *Exactly Solvable Models in Statistical Mechanics* (Academic Press, London, 1982).

[14] M.S. Gronsleth, T.B. Nilssen, E.K. Dahl, E.B. Stiansen, C.M. Varma, A. Sudbo, *Thermodynamic properties near the onset of loop-current order in high-Tc superconducting cuprates*, Phys. Rev. B **79**, 094506 (2009).

[15] A. Giuliani, V. Mastropietro, *Anomalous universality in the anisotropic Ashkin-Teller model*, Comm. in Math. Phys. **256**, 681 (2005); V. Mastropietro, *Non-Perturbative Renormalization* (World Scientific, London, 2008).

[16] S. Wiseman, E. Domany, *Critical behavior of the random-bond Ashkin-Teller model: A Monte Carlo study*, Phys. Rev. E **51**, 3074 (1995).

[17] C. Fan, *On critical properties of the Ashkin-Teller model*, Phys. Lett. **39A**, 136 (1972).

[18] D. Jeziorek-Knioła, G. Musiał, L. Dębski, J. Rogiers, S. Dylak, *On Non-Ising Phase Transitions in the 3D Standard Ashkin-Teller Model*, Acta Phys. Polon. A **121**, 1105 (2012).

[19] D. Jeziorek-Knioła, G. Musiał, Z. Wojtkowiak, *Arbitrarily Weak First Order Phase Transitions in the 3D Standard Ashkin-Teller Model by MC Computer Experiments*, Acta Phys. Polon. A **127**, 327 (2015).

[20] G. Musiał, L. Dębski, G. Kamieniarz, *Monte Carlo simulations of Ising-like phase transitions in the three-dimensional Ashkin-Teller model*, Phys. Rev. B **66**, 012407 (2002).

[21] G. Szukowski, G. Kamieniarz, G. Musiał, *Verification of Ising phase transitions in the three-dimensional Ashkin-Teller model using Monte Carlo simulations*, Phys. Rev. E **77**, 031124 (2008).

[22] W. Janke, *Monte Carlo methods in classical statistical physics*, Lect. Notes in Phys. **739**, 79 (2008).

[23] W. Janke, [In:] *Computer Simulations of Surfaces and Interfaces*, ed. by B. Dünweg, D.P. Landau, A.I. Milchev, NATO Science Series, II. Math. Phys. Chem. **114**, 111–136 (2003).

[24] K. Binder, *Applications of Monte Carlo methods to statistical physics*, Rep. Prog. Phys. **60**, 487 (1997).

[25] M. Mueller, W. Janke, D.A. Johnston, *Nonstandard finite-size scaling at first-order phase transitions*, Phys. Rev. Lett. **112**, 200601 (2014).

Dorota Jeziorek-Knioła was born in 1968 in Pleszew, Poland. She received the Master of Science degree in Physics in 1992 at University in Opole. PhD student in the Computational Physics Division at the Adam Mickiewicz University in Poznań. She is the physics teacher in the 3rd High School in Kalisz and author of many publications in the field of teaching physics at school, as well as 4 scientific publications concerning mainly the Ashkin-Teller model.

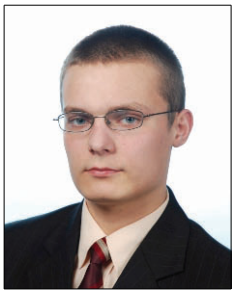

Zbigniew Wojtkowiak was born in 1989 in Śrem, Poland. He has got the Master of Science degree in Biophysics in 2013 at the Adam Mickiewicz University in Poznań. From then on a PhD student at the same University in the Computational Physics Division. In his research he concentrates on numerical simulations and parallel Monte Carlo algorithms for classical spin systems. Moreover, he actively participates in the popularization of science. He is an author of 3 scientific papers.

Grzegorz Musiał was born in Białożewin, Poland, in 1955. He has got the Professor position at the Faculty of Physics, Adam Mickiewicz University in Poznań, Poland. In his research he combines physics and computing. Recently, his research work in physics concentrates mainly on many aspects of statistical physics in classical and quantum spin-lattice systems using numerical simulations. The computing research mainly concerns operating systems of the UNIX type and parallel computing in distributed environment, also with high heterogeneity. He is an author of 64 scientific papers and 5 books.